Three-dimensional parallel edge-based finite element modeling of electromagnetic data with field redatuming

Hongzhu Cai, University of Utah; Martin Čuma and Michael S. Zhdanov, University of Utah, Technoimaging, and MIPT*

Summary

This paper presents a parallelized version of the edge-based finite element method with a novel post-processing approach for numerical modeling of an electromagnetic field in complex media. The method uses an unstructured tetrahedral mesh which can reduce the number of degrees of freedom significantly. The linear system of finite element equations is solved using parallel direct solvers which are robust for ill-conditioned systems and efficient for multiple source electromagnetic (EM) modeling. We also introduce a novel approach to compute the scalar components of the electric field from the tangential components along each edge based on field redatuming. The method can produce a more accurate result as compared to conventional approach. We have applied the developed algorithm to compute the EM response for a typical 3D anisotropic geoelectrical model of the off-shore HC reservoir with complex seafloor bathymetry. The numerical study demonstrates that the modeling algorithm is capable of simulating the complex topography and bathymetry that is commonly encountered in controlled source electromagnetic problems.

Introduction

The development of effective interpretation methods for electromagnetic (EM) survey data requires fast and accurate forward modeling algorithms capable of taking into account the true complexity of the earth geological formation. This is especially important in applications of controlled source EM methods in mineral and oil exploration (Ward and Hohmann, 1988; Zhdanov and Keller, 1994; Constable and Srnka, 2007; Um and Alumbaugh, 2007; Andréis and MacGregor, 2008; Zhdanov, 2009; Zhdanov, 2010; Cai et al., 2014; Zhdanov, 2010).

The finite element method is one of the most flexible to model the complex geoelectrical structures (Schwarzbach et al., 2011; Puzyrev et al., 2013; Cai et al., 2014). In the recent years, the edge-based finite element method, which was originally introduced by Nédélec (1980), gained the interests of the geophysical community for 3D modeling of the EM fields (Silva et al., 2012; Cai et al., 2014). The edge element approach is characterized by better properties, such as automatic enforcement of tangential field continuity and divergence free condition, for the simulating of electromagnetic field compared to the conventional node-based finite element method (Jin, 2002).

This paper introduces a linear edge-based finite element method for EM modeling using unstructured tetrahedral mesh in a general 3D and anisotropic medium. Instead of using the conventional method to compute the scalar components of the field, we present a novel approach for projecting the tangential electric field along the edge to the *x*, *y* and *z* components of the fields on the edge. The method is based on the redatuming technique of electromagnetic data introduced by Cai and Zhdanov (2013). For EM modeling, the tangential field along the edge can be computed on the earth's surface and/or seafloor (in case of marine EM). The tangential field on the surface, where the EM receiver is placed, can be used to recover the EM field underground on a horizontal plane by solving the linear redatuming equations introduced by Cai and Zhdanov (2013). The underdetermined linear system of equations can be solved efficiently in the least square sense. Once the field on the horizontal plane is estimated, one can use it to recompute the scalar components of the field on the surface. We solve the sparse edge-based finite element system of equations using two different multifrontal direct solvers on a cluster with multiple nodes. The direct solvers show higher numerical accuracy and robustness for the ill-conditioned system of equations over iterative solvers based on the Krylov subspace method. The developed algorithm was tested for a 3D off-shore reservoir model with complex seafloor bathymetry. For this complex model, we also consider multiple exciting sources to illustrate the effectiveness of the direct solvers.

Edge-based finite element analysis for the tetrahedral mesh

Compared to the conventional node-based finite element methods which use scalar basis functions defined on the element nodes, the edge-based finite element methods adopt the vector basis functions defined on the center of the element. The computation domain is usually discretized using either structured (such as rectangular bricks) or unstructured (such as tetrahedral) mesh (Cai et al., 2014). The unstructured tetrahedral element is preferred to represent complex geometry and reduce the number of degrees of freedom without losing accuracy.

Figure 1 is an illustration of a tetrahedral element with node and edge indexing. From the figure, one can see that a direction is assigned to each edge and it points from one node to another. We denote the linear node basis functions as $(L_1^e, L_2^e, L_3^e, L_4^e)$.

Three-dimensional edge-based finite element modeling

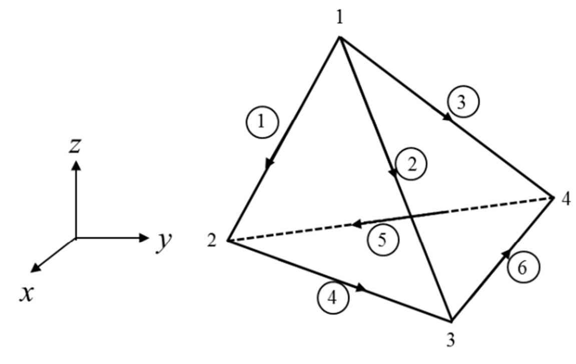

Figure 1: Tetrahedral element with edge and node definition.

It is shown by Jin (2002) that the vector basis function for each edge can be represented by the node basis function as follows:

$$\mathbf{N}_i^e = \left(L_{i_1}^e \nabla L_{i_2} - L_{i_2}^e \nabla L_{i_1}\right) l_i^e \quad (1)$$

where i_1 and i_2 are the first and second nodes connected to the i^{th} edge; l_i^e is the length of the edge.

The electric field is defined at the center of each edge and is denoted as E_i^e. The field inside the tetrahedral element can be represented by the following equation:

$$\mathbf{E}^{\mathrm{e}} = \sum_{i=1}^{6} \mathbf{N}_i^e E_i^e \quad (2)$$

It is easy to verify that the vector edge basis functions are divergence free but not curl free:

$$\nabla \cdot \mathbf{N}_i^e = 0, \nabla \times \mathbf{N}_i^e \neq \mathbf{0}. \quad (3)$$

The vector basis functions are also continuous at the element boundaries. As a result, the divergence free condition of the electric field in source free region and the continuity conditions are imposed directly in the edge-based finite element formulation (Jin, 2002, Cai et al., 2014).

The total field is decomposed into background, $\mathbf{E}^b$, and anomalous fields to avoid the source singularity problem:

$$\mathbf{E} = \mathbf{E}^b + \mathbf{E}^a, \quad (4)$$

The anomalous electric field satisfies to the following equation (Zhdanov 2002, 2009):

$$\nabla \times \nabla \times \mathbf{E}^a - i\omega\mu\widehat{\boldsymbol{\sigma}}\mathbf{E}^a = i\omega\mu\Delta\widehat{\boldsymbol{\sigma}}\mathbf{E}^b, \quad (5)$$

where $\widehat{\boldsymbol{\sigma}} = \widehat{\boldsymbol{\sigma}}_b + \Delta\widehat{\boldsymbol{\sigma}}$ is the conductivity tensor; $\widehat{\boldsymbol{\sigma}}_b$ and $\Delta\widehat{\boldsymbol{\sigma}}$ are the background and anomalous conductivity tensors, respectively.

By substituting equation (2) into equation (5), and using Galerkin's method, one can find the weak form of the original differential equation as follows:

$$\int_\Omega \mathbf{N}_i \cdot [\nabla \times \nabla \times \mathbf{E}^a - i\omega\mu\widehat{\boldsymbol{\sigma}}\mathbf{E}^a - i\omega\mu\Delta\widehat{\boldsymbol{\sigma}}\mathbf{E}^b] dv = 0 \quad (6)$$

where Ω is the modeling domain.

The electric field $\mathbf{E}^a$ can be represented for each element by its tangential value on the edge using equation (2). The background field $\mathbf{E}^b$ can be represented in a similar way.

After applying the first vector Green's theorem, one can find the discretized form of equation (6) for each element:

$$\sum_{e=1}^{N_e} [K^e E_a^e - i\omega\mu M^e \widehat{\boldsymbol{\sigma}}_e E_a^e] - i\omega\mu \sum_{e=1}^{N_e} \sum_{k=1}^{4} \mathbf{N}_i \cdot \left(\Delta\widehat{\boldsymbol{\sigma}}_e L_i^e \left(E_{xi}^e, E_{yi}^e, E_{zi}^e\right)^T\right) = 0, \quad (7)$$

where K^e and M^e are the local stiffness matrices defined as follows (Jin, 2002; Cai et al., 2014):

$$\boldsymbol{K}_{ij}^e = \int_{\boldsymbol{\Omega}_e} (\nabla \times \mathbf{N}_{\boldsymbol{i}}^{\boldsymbol{e}}) \cdot (\nabla \times \mathbf{N}_{\boldsymbol{j}}^{\boldsymbol{e}})\, dv, \quad (8)$$

$$\boldsymbol{M}_{ij}^e = \int_{\boldsymbol{\Omega}_e} \mathbf{N}_{\boldsymbol{i}}^{\boldsymbol{e}} \cdot \mathbf{N}_{\boldsymbol{j}}^{\boldsymbol{e}}\, dv, \quad (9)$$

and Ω_e indicates the domain for one element. The integrals in equations (8) and (9) can be calculated analytically for the tetrahedral and the second term on the left hand side of equation (7) can be evaluated efficiently by using Gauss quadrature (Jin, 2002).

The linear system of equations obtained by assembling the local element matrices can be solved efficiently using either modern direct or iterative solvers.

Multifrontal solver for a linear system of equations

The direct methods for the solution of the linear system of equations have been widely used in numerical applications. These methods are based on the decomposition of the matrix into a lower triangular and upper triangular form:

$$\mathbf{A} = \mathbf{LU} \quad (10)$$

Once the matrix A is decomposed, the solution of the linear system of equations can be obtained by using the forward and backward substitution method (Ascher et al., 2011). The direct methods are known for their numerical accuracy and robustness but are also characterized by high memory consumption and large amount of computation (Ascher et al., 2011). As such, they are often avoided in the 3D modeling of the EM problem. The right-hand side of the finite element system of equations represents the EM excitation source. Once the matrix A is decomposed using the direct method, the decomposed matrix can be reused in the case of multiple-source problem. For iterative solvers, the multiple-source modeling problem needs to be solved separately for each source.

In recent years, with advances in computer technology and algorithmic developments, the direct solvers are being reconsidered for solving the 3D EM modeling problem (e.g., Streich, 2009). The modern direct solvers are based on multifrontal factorization of the stiffness matrix. The two most popular multifrontal solver libraries are MUMPS (Amestoy et al., 2001; 2006) and PARDISO (Schenk et al., 2001). In this paper, we will use these libraries to solve the linear system of equations and compare their performance.

Redatuming of the anomalous EM field

Once the projection of the anomalous field, E_a, along the edge of the tetrahedral is found, the corresponding *x*, *y* and

z components of the field can be obtained either inside the element or on the edge by using the following equation:

$$\mathbf{E}_a^e = \sum_{i=1}^{6} \mathbf{N}_i^e E_{ai}^e. \tag{11}$$

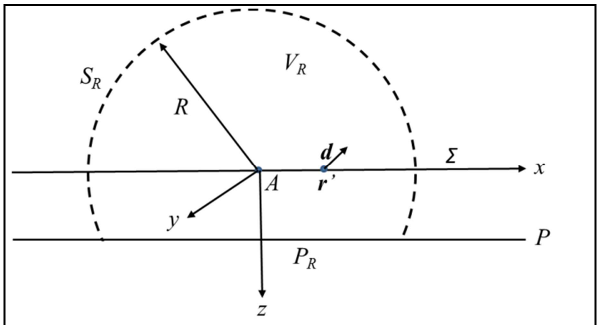

Figure 2: An illustration of redatuming for a typical CSEM survey.

If the scalar components of the field are computed on the edges, the proper weighting functions should be applied since the edges may be shared by several tetrahedrons (Mukherjee and Everett, 2011). For one edge shared by several tetrahedrons, the scalar components of the field computed on the edge from each tetrahedral using equation (11) usually are different from each other since only the tangential continuity along the edge is imposed in the edge-based finite element formulation. As such, the scalar components of the field computed by this method could be very noisy, especially for the linear basis (Jin, 2002).

Redatuming is a new concept introduced by Cai and Zhdanov (2013) for solving the upward and downward continuation problem of the electromagnetic field based on the Stratton-Chu type integrals (Zhdanov, 1988). This method can be extended to the application of the interpolation of the electromagnetic field.

Let us consider a typical electromagnetic survey with the transmitter located at some point A and the receivers distributed over the surface $\sum$ at points with the radius-vector $\mathbf{r}'$ (Figure 2). We introduce a horizontal plane P located at some depth underground (with the axis z directed downward). We also assume that the background conductivity of the earth is given as $\sigma_b(\mathbf{r})$; the domain with anomalous conductivity is below plane P. Let us consider a semisphere, S_R, in the upper half-space with a center located at the transmitter, point A, and a radius R. We will denote the domain bounded by this semisphere and a part P_R, of the horizontal plane P, as V_R. According to Cai and Zhdanov (2013), one can write:

$$\mathbf{d} \cdot \mathbf{E}^a(\mathbf{r}') = \iint_P \{[\mathbf{E}^d(\mathbf{r}'|\mathbf{r}) \times \mathbf{H}^a(\mathbf{r})] - [\mathbf{E}^a(\mathbf{r}'|\mathbf{r}) \times \mathbf{H}^d(\mathbf{r})]\} \cdot d\boldsymbol{s}, \tag{12}$$

where the field $\{\mathbf{E}^d,\ \mathbf{H}^d\}$ is a background field generated in the model with background conductivity by electric dipole with unit moments $\mathbf{d}$, located at a point with the radius-vector $\mathbf{r}'$, $\mathbf{j}^d = \mathbf{d}\delta(\mathbf{r} - \mathbf{r}')$, where δ is a delta function.

Suppose that R→∞ and **d** is a unit vector on the surface where the receivers are distributed. From equation (12), one can see that the EM field on the surface in the direction denoted by **d** can be obtained if we know the distribution of the EM field on plane P.

In a general case, the EM field on plane P is unknown while the EM field on the surface Σ (which can be the earth's surface or seafloor) is given, since the EM receivers are distributed on this surface. In such case, one can solve the inverse problem of equation (12) to estimate the EM field behavior on plane P (Cai and Zhdanov, 2013). Once the field is estimated on plane P, one can use equation (12) to re-compute the field on the surface Σ but in a much denser receiver distribution and in an arbitrary direction.

We consider that the receiver orientation denoted by the unit vector **d** is in an arbitrary direction which is the same as the direction of the edges of the element on the surface. The tangential field along the edge on the surface (seafloor) will be used to estimate $\mathbf{E}_\tau^{Pa}$ and $\mathbf{H}_\tau^{Pa}$ by solving an inverse problem (Cai and Zhdanov, 2013). Finally, we will use equation (12) to recompute the x and y components of the electric field on the surface by setting the unit vector **d** orientation in the x and y directions.

Offshore hydrocarbon reservoir model with complex seafloor bathymetry

The developed algorithm was applied to an anisotropic 3D reservoir model with complex seafloor bathymetry, which is shown in Figure 3. The three-layered background is formed by air, 1000 m thick seawater, and marine sediments. The conductivities of air and seawater are set to be 10^{-6} S/m, and 3.3 S/m respectively.

In this model, the following horizontal and vertical conductivities of the marine sediments were used: $\sigma_h = \sigma_x = \sigma_y = 1\ \mathrm{S/m}$, $\sigma_z = 0.8\ \mathrm{S/m}$. The horizontal and vertical conductivities of the reservoir are set to the following values: $\sigma_{ah} = \sigma_{ax} = \sigma_{ay} = 0.05\ \mathrm{S/}$, $\sigma_{az} = 0.005\ \mathrm{S/m}$, respectively.

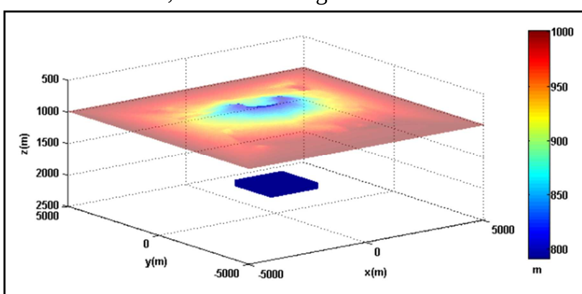

Figure 3: A 3D reservoir model with a complex seafloor bathymetry indicated by the surface. The blue zone under the surface indicates the 3D reservoir. The color scale represents only the elevation of the bathymetry.

We use seven dipole sources for this model to demonstrate the effectiveness of the direct solvers for the problem with multiple right-hand sides. The sources are located at y=0 and z=-600 m. The computation domain is discretized into a 3D unstructured mesh with 5 million elements and 5.9 million edges. Figure 4 shows a 3D view of the tetrahedral mesh for the part of y<0 generated by COMSOL. The receivers are placed directly above the seafloor bathymetry. To better simulate the bathymetry and to ensure high accuracy results on the receivers, we refined our mesh around the receivers and bathymetry region.

Figure 5 shows the total field for these 7 different sources. This larger model is well suited for the parallel scaling analysis that we performed on up to 16 nodes. Table 1 shows the runtime and parallel scaling for both MUMPS and MKL PARDISO, from which it can be seen that the MKL outperforms the MUMPS by about 20%. We have also observed parallel scaling deterioration after 4 nodes, which was caused by decreased local problem size and increased communication needs.

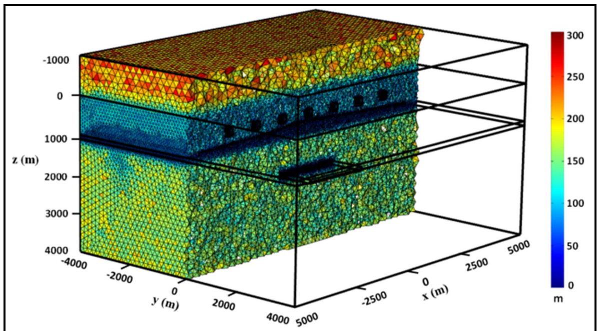

Figure 4: A 3D view of the unstructured tetrahedral element for the part of y<0.

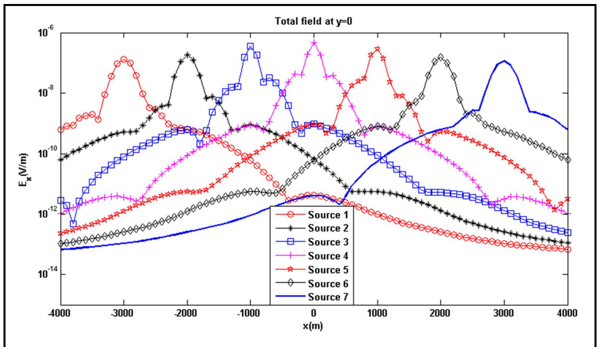

Figure 5: Total field for all 7 different sources.

Table 1: Runtime and parallel scaling of MKL PARDISO (MP) and MUMPS (MU) for the 3D reservoir model

	Runtime [sec]			Parallel scaling	
Nodes	MP	MU	MP/MU	MP	MU
1	1098.64	1255.79	0.87	1.00	1.00
4	467.78	581.50	0.80	2.35	2.16
8	343.89	421.24	0.82	3.19	2.98
12	307.52	309.16	0.99	3.57	4.06
16	297.82	327.97	0.91	3.69	3.83

Conclusions

We have developed an edge-based finite element algorithm for 3D marine CSEM modeling in an anisotropic medium. We consider the Nédélec element with fully unstructured tetrahedral mesh. Two different parallel multifrontal algorithms were used to solve this problem. Numerical results show that the multifrontal direct solvers were accurate and robust for the ill-conditioned system of equations. The direct solver also works efficiently for solving CSEM problems with multiple transmitters. We have also introduced a novel approach of projecting the tangential field along the edge to the scalar component of the field. The resulting method is based on the redatuming theory of electromagnetic field and Stratton-Chu type integral.

The developed algorithm was tested on a model of an off-shore HC reservoir in the presence of a complex bathymetry. The edge-based finite element solutions of these models shows a good agreement with the analytical solution and the integral equation solution. The numerical results also demonstrate that the proposed redatuming method for post-processing of the finite element solution is more accurate than the conventional method. Thus, we conclude that the developed forward modeling algorithm is capable of simulating complex bathymetry in CSEM modeling.

Acknowledgements

The authors acknowledge the support of the University of Utah's Consortium for Electromagnetic Modeling and Inversion (CEMI) and of TechnoImaging. We thank the Center for High Performance Computation at the University of Utah for allocation of the PC cluster resources.

Three-dimensional parallel edge-based finite element modeling of electromagnetic data with field redatuming

References

Amestoy, P. R., I. S. Duff, J. Koster, and J. L'Excellent, 2001, A fully asynchronous multifrontal solver using distributed dynamic scheduling: SIAM Journal of Matrix Analysis and Applications, 23, 15-41.

Amestoy, P. R., A. Guermouche, J. L'Excellent, and S. Pralet, 2006, Hybrid scheduling for the parallel solution of linear systems: Parallel Computing 32,136-156.

Andréis, D., and L. MacGregor, 2008, Controlled-source electromagnetic sounding in shallow water: Principles and applications: Geophysics, 73, F21--F32.

Ascher U. M., and C. Greif, 2011, A first course in numerical methods: SIAM

Constable, S., and L. J. Srnka, 2007, An introduction to marine controlled-source electromagnetic methods for hydrocarbon exploration: Geophysics, 72, WA3--WA12.

Cai, H., and M. S. Zhdanov, 2013, Redatuming of borehole-to-surface electromagnetic data at the Kevin Dome exploration site, 83th Annual International Meeting, SEG, Expanded Abstracts, 685-689.

Cai, H., B. Xiong, M. Han, and M. S. Zhdanov, 2014, 3D controlled-source electromagnetic modeling in anisotropic medium using edge-based finite element method: Computers & Geosciences, 73, 164-176.

Jin, J., 2002, Finite element method in electromagnetics: Wiley-IEEE Press.

Mukherjee, S., and M. E. Everett, 2011, 3D controlled-source electromagnetic edge-based finite element modeling of conductive and permeable heterogeneities: Geophysics 76 (4), F215-F226.

Nédélec, J. C., 1980, Mixed finite elements in R^3: Numerische Mathematik, 35, 315--341.

Puzyrev, V., J. Koldan, J. Puente, G. Houzeaux, M. Vázquez, and J. M. Cela, 2013, A parallel finite-element method for three-dimensional controlled-source electromagnetic forward modelling: Geophysical Journal International, 193, 678--693.

Schenk, O., K. Gatner, W. Fichtner, and A. Stricker, 2001, PARDISO: a high-performance serial and parallel sparse linear solver in semiconductor device simulation: Future Generation Computer Systems, 18, 69--78.

Streich, R., 2009, 3D finite-difference frequency-domain modeling of controlled-source electromagnetic data: Direct solution and optimization for high accuracy: Geophysics, 74, F95-F105.

Schwarzbach, C., R. U. Börner, and K. Spitzer, 2011, Three-dimensional adaptive higher order finite element simulation for geo-electromagnetics--a marine CSEM example: Geophysical Journal International, 187, 63--74.

Silva, N. V., J. V. Morgan, L. MacGregor, and M. Warner, 2012, A finite element multifrontal method for 3D CSEM modeling in the frequency domain: Geophysics, 77, E101--E115.

Um, E. S., and D. L. Alumbaugh, 2007, On the physics of the marine controlled-source electromagnetic method: Geophysics, 72, WA13--WA26.

Ward, S. H., and G. W. Hohmann, 1988, Electromagnetic Theory for Geophysical Applications: SEG.

Zhdanov, M. S., 1988, Integral transforms in geophysics: Springer-Verlag

Zhdanov, M. S., and G. Keller, 1994, The geoelectrical methods in geophysical exploration: Elsevier.

Zhdanov, M. S., S. K. Lee, and K. Yoshioka, 2006, Integral equation method for 3D modeling of electromagnetic fields in complex structures with inhomogeneous background conductivity: Geophysics, 71, 333--345.

Zhdanov, M. S., 2002, Geophysical inverse theory and regularization problems: Elsevier.

Zhdanov, M. S., 2009, Geophysical electromagnetic theory and methods: Elsevier.

Zhdanov, M. S., 2010, Electromagnetic geophysics: Notes from the past and the road ahead: Geophysics, 75, A49--A66.